Atmospheric Environment 144 (2016) 146–159

Contents lists available at ScienceDirect

Atmospheric Environment

journal homepage: www.elsevier.com/locate/atmosenv

Accidental benzene release risk assessment in an urban area using an atmospheric dispersion model

Son C.H. Truong, Myong-In Lee*, Ganghan Kim, Dongmin Kim, Jong-Hwa Park, Sung-Deuk Choi, Gi-Hyoug Cho

School of Urban and Environmental Engineering, Ulsan National Institute of Science and Technology (UNIST), Ulsan, Republic of Korea

HIGHLIGHTS

- Risk assessment of atmospheric dispersion of toxic chemicals in the urban area.
- Characteristic patterns of atmospheric dispersion in the anthroposphere
- Risk maps based on multiple AERMOD simulations and indoor and outdoor populations.
- Quite different risk depending on the meteorological condition and population.
- Risk needs to be assessed by chemical concentration and population.

GRAPHICAL ABSTRACT

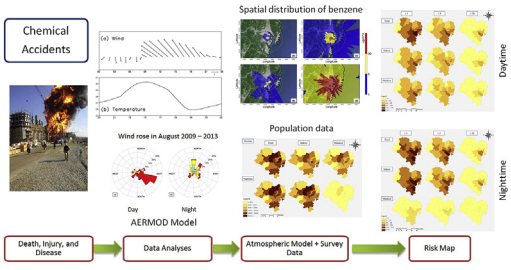

ARTICLE INFO

Article history:
Received 22 February 2016
Received in revised form
23 August 2016
Accepted 28 August 2016
Available online 30 August 2016

Keywords:
Benzene
Accident
AERMOD
Potential risk
Indoor
Outdoor
Population

ABSTRACT

This study applied the American Meteorological Society and Environmental Protection Agency Regulatory Model (AERMOD) to assess the risk caused by an accidental release and dispersion of the toxic chemical benzene in the vicinity of a highly populated urban area. The modeling domain encompasses the Korean megacity of Ulsan, which includes two national industrial complexes and is characterized by a complex coastal terrain. Multiple AERMOD simulations were conducted for an assumed emission scenario using background wind data from August between 2009 and 2013. The series of experiments produced the spatial accident probability patterns for different concentration levels during daytime and nighttime scenarios based on the corresponding dominant wind patterns. This study further quantifies the potential accident risk based on the number of affected individuals by combining the accident probability with the indoor and outdoor population estimates. The chemical gas dispersion characteristics depend on various local meteorological conditions, such as the land-sea breeze direction, which alternates between daytime and nighttime, and the atmospheric stability. The results reveal that benzene dispersion affects a much larger area during the nighttime owing to the presence of a nocturnal stable boundary layer with significant temperature stratification. The affected area is smaller during the daytime owing to decreased stability and enhanced vertical mixing in the boundary layer. The results include a high degree of uncertainty during the nighttime owing to weak wind speeds and the lack of a prevailing wind direction, which impact the vulnerable area. However, vulnerable areas are more effectively identified during the daytime, when more consistent meteorological conditions exist. However, the

* Corresponding author. School of Urban and Environmental Engineering, Ulsan National Institute of Science and Technology, 50 UNIST-gil, Ulju-gun, Ulsan 689-798, Republic of Korea.
E-mail address: milee@unist.ac.kr (M.-I. Lee).

http://dx.doi.org/10.1016/j.atmosenv.2016.08.075

potential risk becomes much lower during the nighttime owing to a substantial reduction of the outdoor population.

1. Introduction

Most metropolitan cities worldwide suffer from serious air quality degradation (Baklanov et al., 2016). Rapid industrialization and urbanization represent major reasons for air quality degradation, resulting in increased air pollutant emissions due to transportation and in energy production and consumption due to industrial activities. These negative environmental impacts are often concentrated in or near densely populated areas. The United Nations (UN) reported that 54% of the world population lived in urban areas in 2014, which is projected to increase to 66% by 2050 (UNWUP, 2014). Urbanization and the associated air quality impacts have become an active research area. Many studies have been conducted to examine the short-term and long-term effects of air pollution on human health in metropolitan areas. Hang et al. (2015) investigated the adverse health impacts caused by nitrogen compounds in major urban areas of South Korea. Gurjar et al. (2010) assessed the health risks, mortality and morbidity caused by sulfur dioxide, nitrogen and total suspended particles in megacities.

Growing concerns exist regarding the accidental release of hazardous materials and explosions in or near megacities. These events can cause more serious short-term health effect and immediate casualties. The Union Carbide pesticide plant accident in Bhopal, India is one well known example. At least 40 tons of the highly toxic methyl isocyanate gas and a number of other poisonous gases were released on the evening of December 2, 1984. Death toll estimates vary from 3800 to 16,000, but the current death toll suggests that 15,000 people have been killed because of the accident, both immediately and over time. After 30 years, toxic material remains in the local environment and many of those who were exposed to the gas have given birth to physically and mentally disabled children (Edward, 2005). A series of massive explosions in the port of Tianjin, China represent another urban accident. The explosions killed 173 people and injured 797 more on August 12–15, 2015. In addition, the explosions caused as much as $1.5 billion USD in damages, making the event the most costly disaster in China in recent years (Huang and Zhang, 2015).

According to the statistical summary from the Korea Research Institute of Chemical Technology (http://eng.me.go.kr/), over 70 chemical accidental events occurred in Korea from 2010 to 2013. These events are associated with various types of carcinogenic chemical compounds, including benzene, hydrochloric acid, ammonia and others (http://stat.me.go.kr/). Such accidents not only kill and injure industrial complex workers but also affect the surrounding residential areas. A notorious accident occurred in Gumi, South Korea on September 27, 2012. Approximately eight tons of highly toxic hydrogen fluoride gas was released from the Hube Global chemical plant. The leak killed 5 workers and injured at least 18 people. The gas spread to the adjacent residential area where 3200 people were treated for nausea, chest pain, rashes and sore eyes after inhaling toxic fumes. The leak also damaged crops and livestock. These sudden hazardous material releases are more likely to instantly kill people and affect nearby urban residential areas (Lim and Lee, 2012; Park, 2013).

Accidental toxic chemical releases and dispersion are now included in urban planning risk assessments owing to growing awareness among policy-making agencies. One proposal seeks to establish the Emergency Alert Systems (EASs) throughout the city (Tseng et al., 2008; Lee et al., 2015). However, high-density monitoring network construction and maintenance can be costly, specifically networks that observe the atmospheric dispersion of hazardous chemicals. Therefore, researchers increasingly utilize various numerical models, which can provide the toxic gas dispersion estimates in near real time (Marcelo et al., 2003; Holmes and Morawska, 2006). These estimates save time during the decision-making and action or evacuation processes. For example, the first all-evacuation order was issued by the municipal office 3 and a half hours after the Gumi accident. However, the order was too late to effectively rescue people and prevent damages. Therefore, the American Meteorological Society and U.S. Environmental Protection Agency Regulatory Model (AERMOD) is applied in this study (Perry et al., 2005).

The AERMOD model has been used in numerous studies, including dispersion analyses for various pollutants, such as PM_{10}, $PM_{2.5}$, NO_x, SO_2, mercury and others (Kanyanee et al., 2011; Kakosimos et al., 2011; Nicole et al., 2011, Hasson et al., 2013; Hadlocon et al., 2015; etc.). AERMOD has also been compared to other models, including the California Puff Model (CALPUFF) and the Atmospheric Dispersion Modeling System (ADMS) (Andler et al., 2012; Tartakovsky et al., 2013; Arthur, 2014; Mark et al., 2015; Tartakovsky et al., 2016), and integrated with the Weather Research and Forecasting (WRF) model to analyze the sensitivity to metrological conditions associated with PM_{10} dispersion calculations (Amit et al., 2007). In addition, AERMOD was used to conduct a health risk assessment of coal-fired power plant emissions, including the carcinogenic and non-carcinogenic health risk associated with both short-term and long-term exposure (Mutahharah et al., 2014).

This study investigates the effects of such accidents on human health based on long-term, multiple dispersion simulation statistics in a region. These statistics can identify high risk potential areas, providing useful information for policy makers and local stakeholders. Ulsan, South Korea is selected as a case study because it is one of the fastest growing urban areas in the nation. The UN estimates that 82% of the South Korean population lives in urban areas (UNWUP, 2014). Benzene is selected as a representative chemical because this represents a first class carcinogenic chemical that is produced in Ulsan industrial complexes. However, the generalized modeling framework utilized in this study can also be used to assess various other applications and gases. The assumed scenario for the accidental benzene release is based on information from past accidents in South Korea.

Long-term simulation statistics are required to create a risk map. Multiple AERMOD simulations were conducted based on different background winds, which were observed at the Ulsan weather station. The benzene concentration 1 h after the emission (i.e., 1-h concentration) and the frequency exceeding a threshold concentration value have been averaged to obtain the spatial distribution of the potential risk method. This method differs from those described in other AERMOD studies (Mutahharah et al., 2014; Silverman et al., 2007) in which only the peak maximum value of 1-h concentration is used for the risk assessment of a given location. The short-term atmospheric dispersion of toxic strongly depends on wind variations and atmospheric stability. Ulsan is located in the coastal region and has a complex terrain. The terrain creates complicated local circulation patterns, including land-sea breeze and mountain-valley

circulation patterns. We also analyze the differences between benzene dispersion events that begin during the daytime and nighttime, adjusting for meteorological condition variations.

In addition, this study quantifies the potential risk based on the number of people affected by the toxic chemical exposure. The number of exposed individuals may differ depending on the local population distribution near an accident site. Moreover, quantitative risk assessments should include people inside and outside of buildings during the exposure period owing to complex population migration patterns in urban areas. Individuals outside are more vulnerable and likely to inhale toxic gases. This study combines the highly concentrated toxic chemical dispersion probability from the long-term AERMOD simulations with the population distribution at the time of the accident. The spatiotemporal distributions in the 56 sub-municipal administrative divisions of the Ulsan Metropolitan City are based on Park et al. (2016), who used these divisions to estimate earthquake casualties.

The investigation was conducted to obtain the following information: 1) the locations where an airborne hazardous material plume is expected to spread based on local circulations and atmospheric stability; 2) the locations with the highest concentrations, as well as daytime and nighttime concentration variations; 3) the toxic benzene concentration levels simulated in each high-risk area; and 4) the potential risk patterns based on the number of individuals affected during a given accident.

Section 2 describes the AERMOD model and experimental design of this study. The simulation results and discussion are presented in Section 3. The concluding remarks are given in Section 4.

2. Methodology

2.1. Study area

The metropolitan city of Ulsan is the seventh largest city in South Korea, encompassing an area of 1057.5 km^2 and population of over 1.142 million in 2015 (http://kostat.go.kr/). The city is located in the southeast portion of the country, neighboring Busan to the south and Gyeongju to the north. The Ulsan metropolitan city includes two national industrial complexes, the Ulsan Petrochemical Industrial Complex and the On-San Industrial Complex. These two industrial complexes produce and treat various industrial products, increasing the potential health risks in nearby residential areas.

Fig. 1 shows a geographic map of the study area, including the emissions point source and nearest meteorological station locations. The emissions point source is assumed to be located at the center of the Ulsan Petrochemical Industrial Complex (35°30′16″N and 129°21′12″E), which is within 3–5 km of heavily populated downtown Ulsan (Fig. 1c).

2.2. Model description

AERMOD is a steady-state, straight-line trajectory plume model. The model assumes that the concentration during a simulated hour is governed by the temporally averaged meteorology during that hour. The time averaged mass concentration is assumed to have the distribution as:

$$C = \frac{Q}{2\pi U\sigma_y\sigma_z}\exp\left(-\frac{1}{2}\frac{y^2}{\sigma_y^2}\right)\left\{\exp\left(-\frac{1}{2}\frac{(z-H)^2}{\sigma_z^2}\right) + \exp\left(-\frac{1}{2}\frac{(z+H)^2}{\sigma_z^2}\right)\right\} \quad (1)$$

where C is the steady-state concentration at a point (x, y, z) in μg m^{-3}; Q is the emission rate in μg s^{-1}; U is the average wind speed (m s^{-1}) at stack height, σ_y and σ_z are the horizontal and vertical spread parameters in meter, respectively; y is the horizontal distance from plume centerline (m); z is the vertical distance from the ground level (m); and H is the effective stack height ($H = h + \Delta h$) with h = physical height, and Δh = plum rise in meter. The mass concentration of pollutant is determined by combined effects of diffusion and advection. The diffusion due to turbulent eddy motion is assumed to be isotropic with the Gaussian distribution, and the advection effect is represented with the wind velocity (U). Therefore the simulated concentration is dominated by advection process when the wind velocity is sufficiently large, whereas it is dominated by diffusion process in the calm or weak wind cases.

The calculation of plum rise Δh is done, depending on the variation of planetary boundary layer (PBL), for the convective boundary layer (CBL):

$$\Delta h_d = \left(\frac{3F_m x}{\beta_1^2 u_p^2} + \frac{3}{2\beta_1^2} + \frac{F_b x^2}{u_p^3}\right)^{1/3} \quad (2)$$

and the stable boundary layer (SBL):

$$\Delta h_s = 2.66\left(\frac{F_b}{N^2 u_p}\right)^{1/3} \times \left[\frac{N' F_m}{F_b}\sin\left(\frac{N' x}{u_p}\right) + 1 - \cos\left(\frac{N' x}{u_p}\right)\right]^{1/3} \quad (3)$$

cases, respectively, where = $F_m$stack momentum flux;F_b = stack buoyant flux;β_1 = 0.6, an entrainment parameter;u_p = wind speed;x = downwind distance; and N (= N'/0.7) Brunt-Vaisala frequency (s^{-1}).

The model uses different dispersion parameters for urban and rural conditions during the nighttime. An empirical model is used to estimate the urban heat island impact, where the urban-rural temperature difference (ΔT_{u-r}) is a function of the population:

$$\Delta T_{u-r} = \Delta T_{max}\left[\left(0.1\ \ln\left(\frac{P}{P_0}\right) + 1.0\right)\right] \quad (4)$$

where = ΔT_{max}12 °C,P_0 = 2,000,000 and P = the population of the area. Sensitivity experiments are conducted in Section 3.2 by changing the urban population to 1,000,000 (N_Urban_1) and 2,000,000 (N_Urban_2). These scenario results are then compared to the results of a scenario with no urban heat island impact (N_Rural). Unless noted, the model used the default value of 1,000,000, which is close to the actual population of Ulsan.

The AERMOD system consists of one main program (AERMOD) and two pre-processors (AERMET and AERMAP). The meteorological preprocessor AERMET provides AERMOD with the meteorological information required to characterize the planetary boundary layer (PBL) parameters, such as the friction velocity, Monin-Obukhov length, convective velocity scale, temperature scale, mixing height and surface heat flux. AERMET requires surface characteristics, cloud cover, and upper air temperature sounding inputs, as well as near surface wind speed, wind direction and temperature measurements. The meteorological data collected at the nearest automated surface observation system (ASOS) station were used for the near surface inputs. Rawinsonde data was observed at Pohang, which is the nearest available site, located 50 km from Ulsan. This data was used for the upper air data, assuming relatively constant wind upper level wind patterns. Additionally, the EPA's Revision to the Guideline on Air Quality Models (U.S. EPA, 2005a) suggests that at least five years of representative meteorological data should be used when estimating general dispersion patterns using an air quality model such as

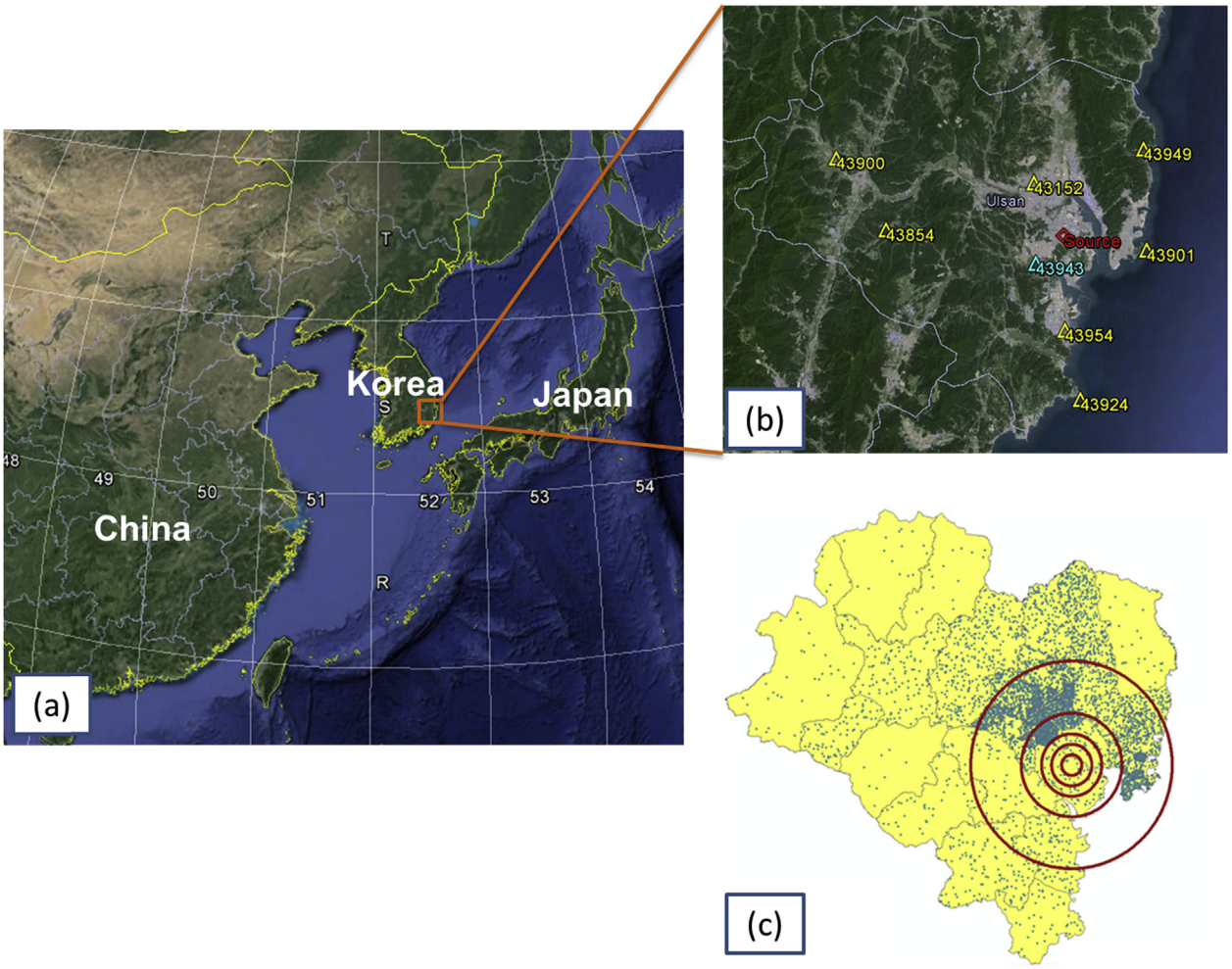

Fig. 1. (a) The geographical location, (b) landscape and (c) population density of Ulsan. The location of the assumed emission source is represented by the red diamond in (b). The location of the automatic weather station used in this study is represented by the cyan triangle, while other nearby stations are represented by yellow triangles with station identification numbers. Each blue dot in (c) represents 200 people. The circles in (c) indicate the areas within 1 km, 2 km, 3 km, 5 km and 10 km of the emission source. The satellite images in (a) and (b) are taken from Google Earth. (For interpretation of the references to colour in this figure legend, the reader is referred to the web version of this article.)

AERMOD. This study focuses on a summer scenario; therefore, only August was studied from 2009 to 2013. Five-year meteorological data were used to analyze year to year variations. The albedo, Bowen ratio and surface roughness were set to 0.16, 2 and 1 m, respectively, based on typical summer urban conditions.

AERMOD simulates a plume as a weighted sum of the concentration based on two scenarios: (i) a horizontal plume under very stable conditions and (ii) an elevation-dependent plume. The topographical effects of the study area were addressed using AERMAP at a resolution of ~90 m. These simulations are based on the Shuttle Radar Topography Mission (SRTM3) database from the U.S. National Geospatial-Intelligence Agency (NGA) and the U.S. National Aeronautics and Space Administration (NASA). The simulations were conducted using a comprehensive Cartesian receptors grid with a 200 m grid spacing to a distance of 20 km from the approximate emission source. Initial concentration of hazardous chemical was set to zero for the entire domain, and the model uses the open boundary condition except the ground where the atmospheric chemical is not allowed to penetrate.

2.3. Experimental design

The emission starting time was set to 0100 LST for the nighttime case and 1300 LST for the daytime case. The benzene emissions from the source lasted for an hour as an assumed scenario. A set of 155 simulations (31 days over 5 years) were conducted to derive the 1-h average ground-level concentrations for each case, which are eventually averaged to determine the mean August concentration for a given day. Benzene is released from a tank that is assumed to be 3 m in diameter and 5 m in height at an emission rate of 94 g s^{-1}. These parameters roughly correspond to the size of an internal floating roof tank (IFRT). IFRTs are commonly used to store chemicals and hazardous materials at the Ulsan Petrochemical Industrial Complex.

Benzene is carcinogenic to humans and no safe level of exposure can be recommended. The airborne benzene concentrations associated with excess lifetime risks of 1/10,000, 1/100,000 and 1/1,000,000 are 17, 1.7 and 0.17 μg m^{-3}, respectively (WHO, 2000). We selected 3 standard thresholds of 30 μg m^{-3}, 5 μg m^{-3} and 1 μg m^{-3} to categorize the risk areas and identify high risk areas. The 30 μg m^{-3} threshold represents a dangerous concentration for benzene inhalation in ambient air as proposed by the Integrated Risk Information System (IRIS: http://www.epa.gov/iris/subst/0276.htm). The 5 μg m^{-3} threshold is based on the European Union Standard (EUS) (Ambient Air Quality Directive, 2008), which proposes human health protective limit values in Annex XI. The 1 μg m^{-3} threshold is selected as the lowest assessment threshold.

Note that our use of AERMOD differs from conventional usage.

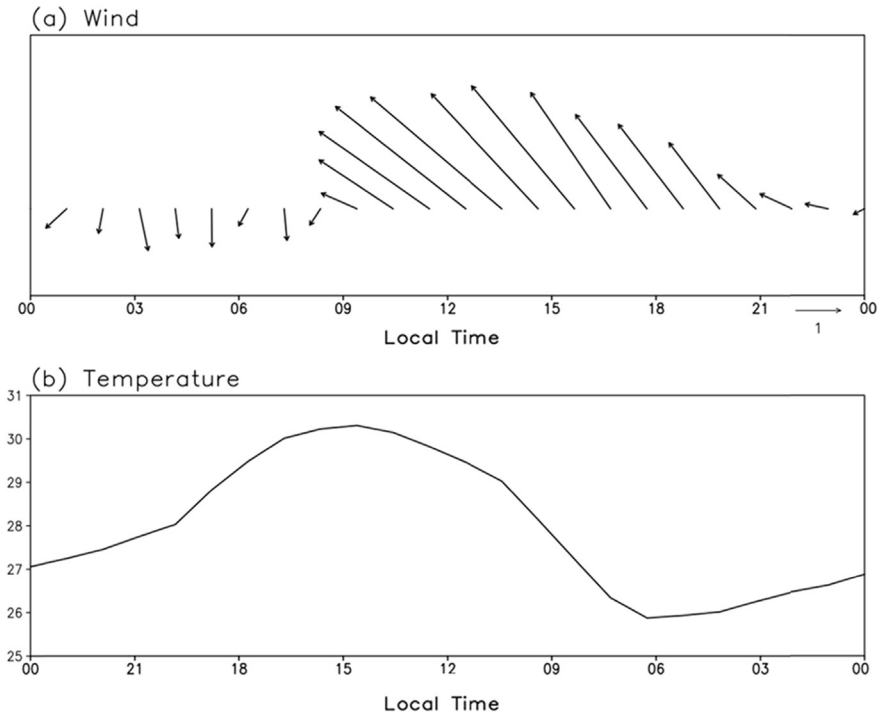

Fig. 2. Diurnal surface (a) wind and (b) temperature variations at the Ulsan weather station in August averaged between 2009 and 2013. The wind direction and speed during each hour of the day are represented by the arrow directions and lengths, respectively, in (a). Easterly (westward) winds are depicted by arrows facing to the left, westerly to the right, southerly upward and northerly downward. The wind speed is scaled based on a reference arrow of 1 m s^{-1} (illustrated at the bottom right hand corner of the figure).

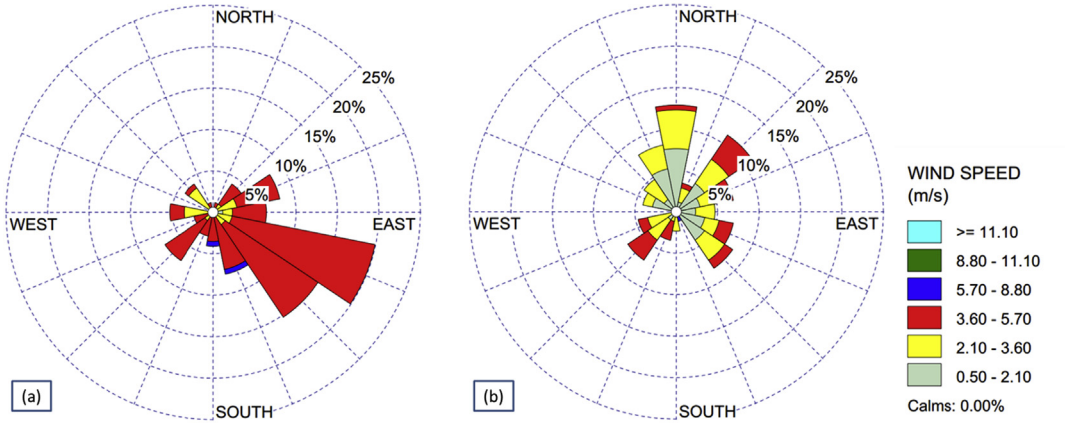

Fig. 3. Wind rose diagrams at (a) 1300 LST and (b) 0100 LST measured at the Ulsan weather station in August 2009–2013. A total of 155 wind data are used in each figure, representing 31 days over 5 years.

The conventional usage estimates the human health risk at a given location by obtaining the maximum ground-level concentration from the simulations at a given point (Mutahharah et al., 2014; Silverman et al., 2007). This usage seems adequate for chronic impact assessments associated with long-term exposure to specific air pollutants. However, this usage may not be appropriate for evaluating the spatial risk patterns caused by accidental toxic chemical and hazardous material releases over a short period of time. Therefore, we average the toxic chemical concentrations and assess the risks for a given period of time after the accident occurs.

2.4. Risk assessment

Section 3.4 assesses the adverse human health impacts by defining risk in terms of the number of people affected by the accidental toxic chemical release, as given by:

$$R_i = P_i \times PO_i \quad (5)$$

The risk R in an area i is estimated as the product of the population P in the area and the probability of an accident PO. The risk is assessed in 56 submunicipal administrative divisions in the Ulsan metropolitan city. This study further considers indoor and outdoor population variations at a given location during the daytime and nighttime. The spatiotemporal distribution of the Ulsan population was estimated based on Park et al. (2016) at the administrative division level. This estimate utilizes daily time use empirical survey data collected by Statistics of Korea. AERMOD outputs the

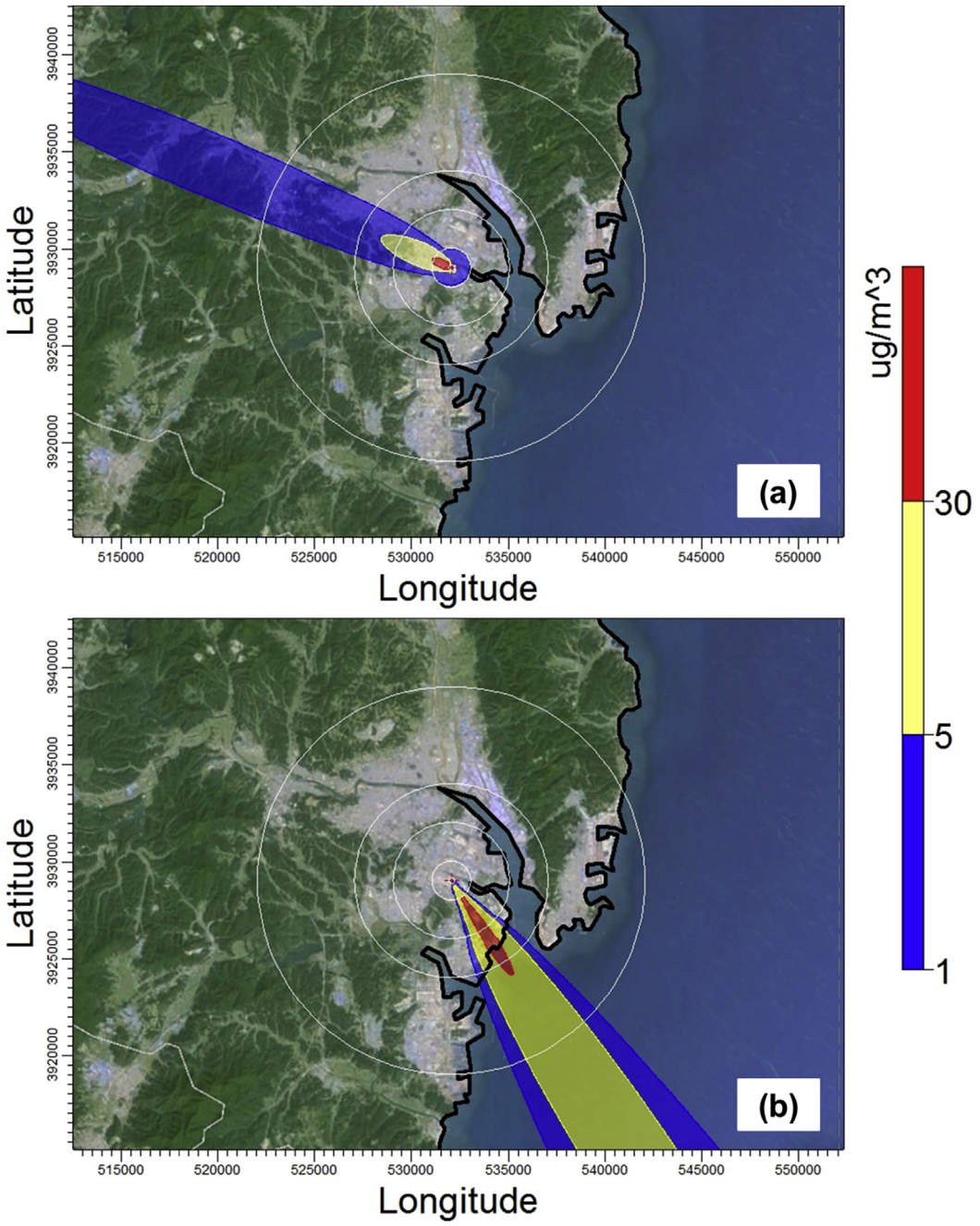

Fig. 4. Spatial distributions of the 1-h average benzene concentration at (a) 1300 LST and (b) 0100 LST on August 15, 2013.

simulated concentrations at each 200 m × 200 m grid square. Therefore, the concentration values within each administrative division are averaged to represent the concentration of that division and the accident probability. The accident probability is considered based on concentration levels exceeding 1, 5 and 30 μg m^{-3}.

3. Results

3.1. Meteorological analysis

Atmospheric toxic chemical dispersion largely depends on the local meteorological conditions of a region, including wind and PBL stability. Fig. 2 shows the diurnal wind and temperature variations in August, which are averaged using long-term observations from 2009 to 2013. The local land-sea breeze circulation clearly affects and reverses the wind direction (Fig. 2a). A southeasterly sea breeze develops between 0900 and 2300 LST, whereas a relatively weak northerly or northeasterly wind exists from 0000 to 0800 LST, corresponding to the land breeze during the nighttime. This land-sea breeze circulation is driven by temperature differences between the land and ocean in the coastal region. The circulation effect is largest when the local land temperature (Fig. 2b) peaks at approximately 1500 LST. The lowest land temperature is observed at approximately 0600 LST and is generally induced by land surface cooling due to nighttime radiation, which is accompanied by a

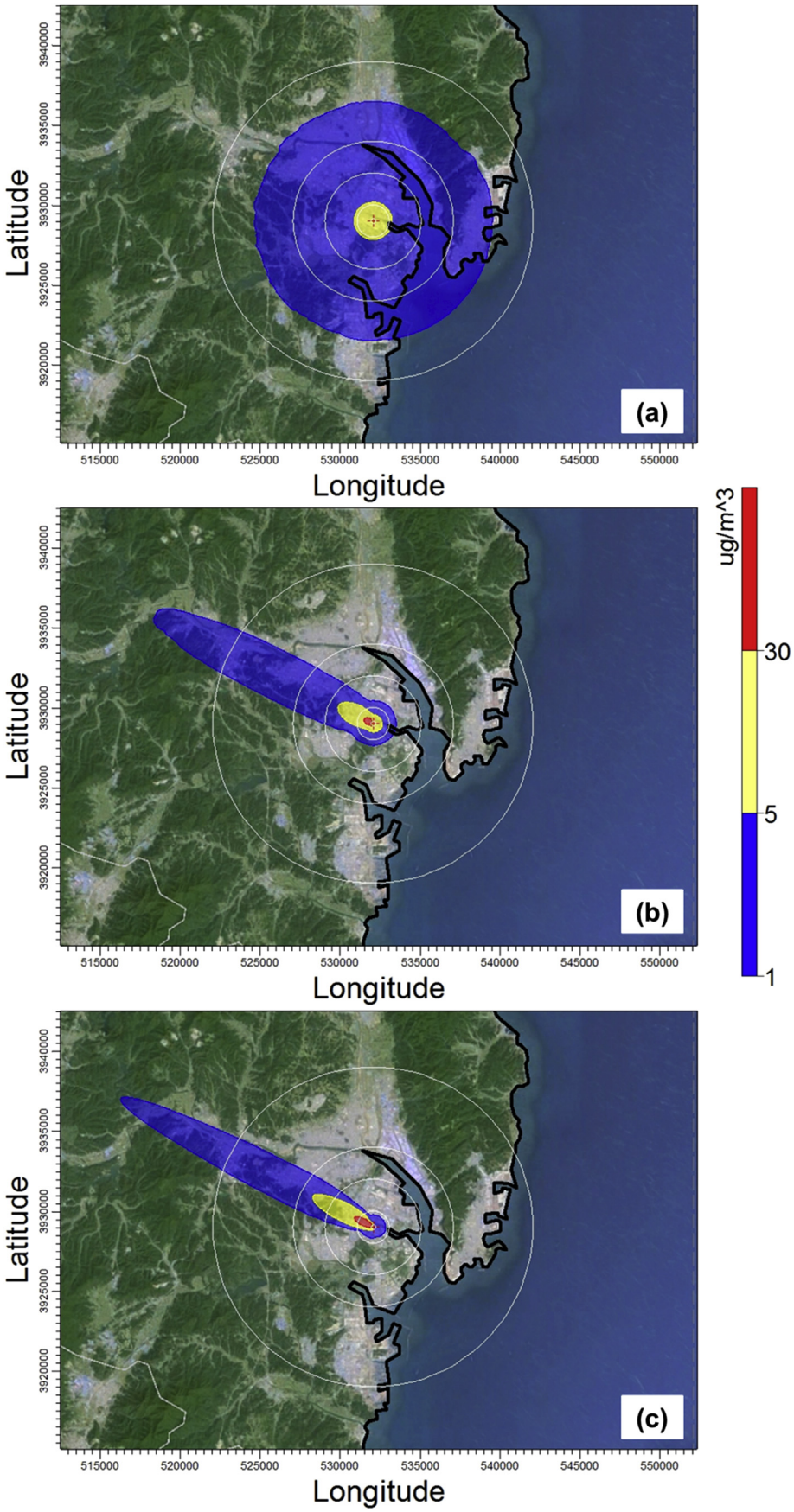

Fig. 5. Spatial distribution of the 1-h average benzene concentration at 1300 LST for wind speeds of (a) 0.5 m s^{-1}, (b) 2.5 m s^{-1} and (c) 5 m s^{-1}.

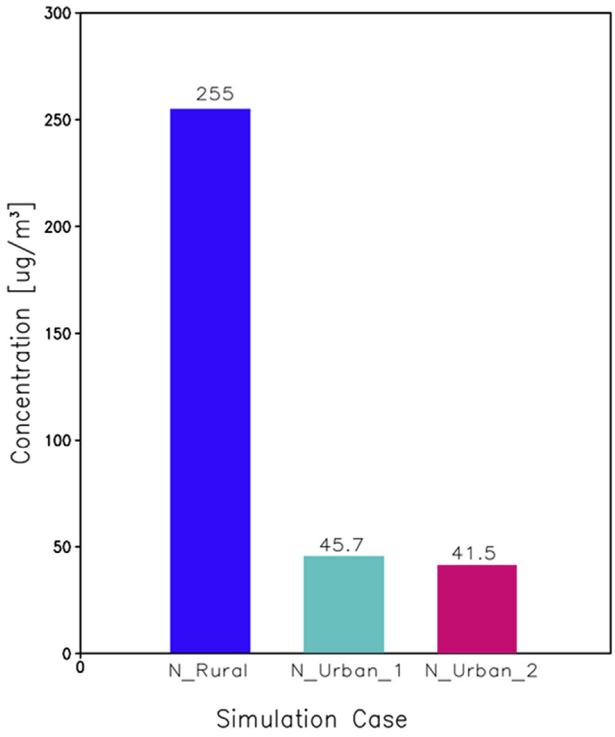

Fig. 6. Differences between the maximum 1-h concentrations via the sensitivity experiments. N_Rural indicates the scenario in which the urban heat island impact is not considered during the nighttime. The N_Urban_1 and N_Urban_2 scenarios include the urban heat island impact based on populations of 1,000,000 and 2,000,000, respectively.

northerly land breeze. The land breeze is less clearly defined in this region compared to the daytime sea breeze.

The toxic chemical dispersion is not affected by time-averaged wind patterns, but is impacted by daily wind direction and speed variations. The wind speed variations are described using the wind speed analysis in Fig. 3, which compares daytime and nighttime hourly wind observations from August 2009 to 2013. The wind observations at 1300 LST and 0100 LST were selected to represent the typical daytime and nighttime patterns, respectively. The results also demonstrate that the degree to which the wind speed and direction varies for a given time of a day, primarily due to daily weather changes. The average daytime wind speed is 4.01 m s^{-1}, and 69% of the wind observations fall within the range of 3.6–5.7 m s^{-1} (Fig. 3a). The prevailing daytime wind distribution is dominated by southeasterly winds. The average inland wind speeds are much stronger than the coastal wind speeds. Note that a southeasterly wind prevails for the 3.6–5.7 m s^{-1} wind class, whereas no prevailing wind direction exists for the weaker wind class of 2.1–3.6 m s^{-1}. This result suggests that the typical sea breeze magnitude in Ulsan is approximately 3.6–5.7 m s^{-1}. The nighttime surface wind speed decreases, averaging 2.56 m s^{-1}, or approximately 64% of the daytime wind speed. The dominant wind speed classes range from 2.1 to 3.6 m s^{-1} and 0.5–2.1 m s^{-1}, accounting for approximately 37.4% and 36.8% of the total cases, respectively. In addition, the nocturnal wind in Ulsan does not exhibit a prevailing direction. However, the 2.1–3.6 m s^{-1} class winds exhibit a slight northerly trend, presumably indicating the typical land breeze wind speed in this location. The wind rose diagram also illustrates significant percentages of northeasterlies, southwesterlies and even southeasterlies in the higher wind range of 3.6–5.7 m s^{-1}.

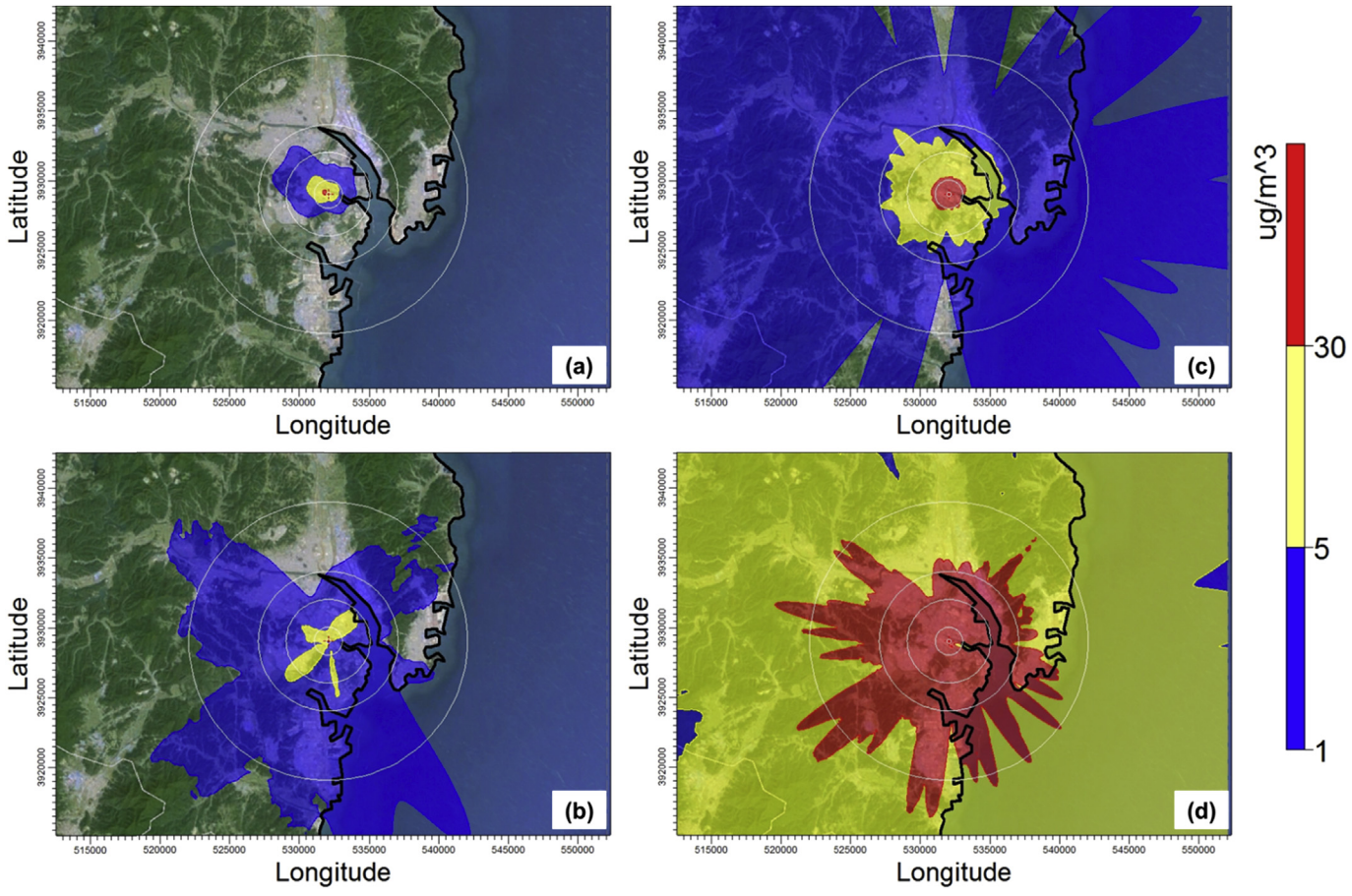

Fig. 7. Comparison between the average and highest 1-h benzene concentration obtained from the multiple simulations conducted in August 2009–2013. (a) and (b) illustrate the average distributions for the daytime (1300 LST) and the nighttime (0100 LST), respectively. (c) and (d) are the same as (a) and (b), but illustrate the highest concentrations.

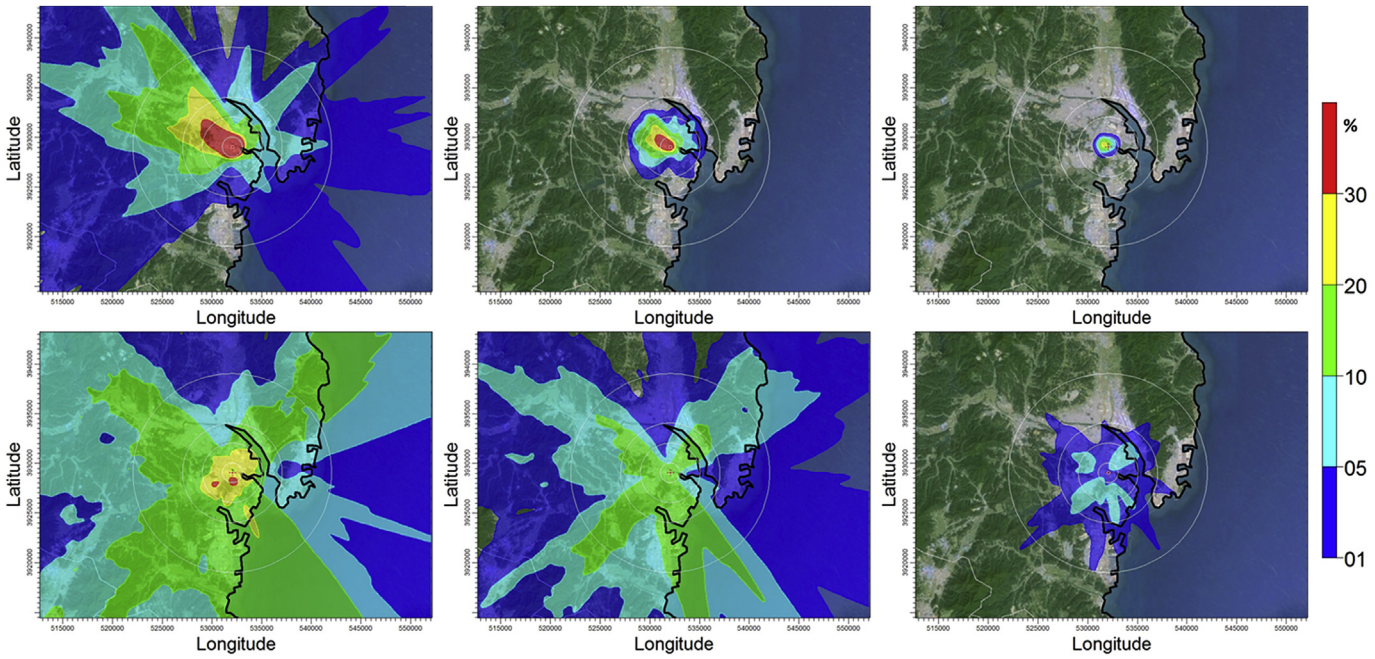

Fig. 8. Spatial distribution of probability that the 1-h average benzene concentration exceeds 1, 5 and 30 μg m^{-3} in August (from left to right) based on the assumed emissions during the daytime (upper) and the nighttime (lower).

Comparing the results illustrated in Figs. 2 and 3 suggests that the local wind plays an important role in toxic chemical dispersion. The dispersion characteristics should not be simply surmised based on the prevailing wind, such as dispersion estimated using the time-averaged wind in a region. Dispersion analyses should consider actual wind direction and magnitude variations. The prevailing wind illustrated by the wind rose diagram (Fig. 3a) is consistent with the daytime time-averaged wind in Fig. 2. However, the nocturnal wind displays no prevailing wind direction or speed, which is quite difficult to ascertain from Fig. 2. This result justifies our approach, which combines the results from multiple dispersion simulations conducted with various wind forcing.

3.2. Dispersion characteristics

Fig. 4 compares the 1-h average concentration results after the assumed benzene release at 1300 LST and 0100 LST on August 15, 2013, illustrating both the daytime and nighttime cases. Both simulations illustrate the typical simple Gaussian dispersion plume pattern simulated by AERMOD. The area affected by a concentration over 30 μg m^{-3} (red contours in the figure) is smaller for the daytime case. The high concentration region is confined within 1.2 km of the source region during the daytime. However, the high concentration region expands from 2 km to over 5 km during the nighttime based on the wind direction. Despite displaying a smaller high concentration region, the maximum daytime concentration is higher than the maximum nighttime concentration. The concentration averaged over the high concentration region is 46 μg m^{-3} during the daytime and 36 μg m^{-3} during the nighttime. The maximum concentration value is 79 μg m^{-3} in Fig. 4a and 46 μg m^{-3} in Fig. 4b. Stronger daytime turbulence mixing vertically diffuses the plume. Thus, the plume is more likely to reach the ground at a higher concentration level and the maximum concentration location is generally situated closer to the emission source during the daytime (Silverman et al., 2007).

The background wind speed also affects the dispersion characteristics (Kanyanee et al., 2011). The 4.01 m s^{-1} daytime wind speed is higher than the 2.56 m s^{-1} nighttime wind speed, leading to a higher maximum ground concentration ground near the emission source. This result can be explained by the AERMOD formulation (Alan et al., 2005), in which the maximum ground level concentration of a gaseous pollutant is inversely proportional to the square of the effective stack height as in Eq. (1), which is inversely proportional to the wind speed as in Eqs. (2) and (3). Therefore, a higher wind speed tends to produce a larger simulated maximum concentration by decreasing the plume rise parameter. Daytime wind speed variation sensitivity experiments were conducted at levels of 0.5, 2.5 and 5 m s^{-1} to clarify this result. Other model settings were unchanged. Fig. 5 compares that the benzene concentrations at the ground based on various wind speeds. The maximum concentration near the emission source tends to increase as the wind speed increases. In fact, higher wind speeds increase both the maximum concentration (e.g., concentrations of 27, 48 and 88 μg m^{-3} for wind speeds of 0.5, 2.5 and 5.0 m s^{-1}, respectively) and the ground concentration in all of the downstream regions. These results confirm that stronger winds generate less vertical plume displacement, favoring long distance horizontal transport with increased ground-level concentrations (Amit et al., 2007). The wind speed in AERMOD must be greater than 0.5 m s^{-1} to induce horizontal plume dispersion. However, chemical gases are less vertically diluted at night owing to the strong PBL stability and turbulence suppression. These characteristics favor horizontal transport and influence larger areas, even though low wind speeds increase the plume rise parameter.

Another sensitivity experiment was conducted to analyze the daytime and nighttime variations associated with the urban heat island parameters in AERMOD. Fig. 6 illustrates that the highest 1-h concentration in the domain significantly varies during the nighttime simulations when the urban heat island parameter changes. The maximum concentration decreases from 255 μg m^{-3} to 45.7 μg m^{-3} when the urban heat island option is changed from rural to urban. The maximum concentration further decreases from 64.4 μg m^{-3} during the N_Urban_1 run to 41.5 μg m^{-3} during the N_Urban_2 run, as the population increases per Eq. (4). AERMOD

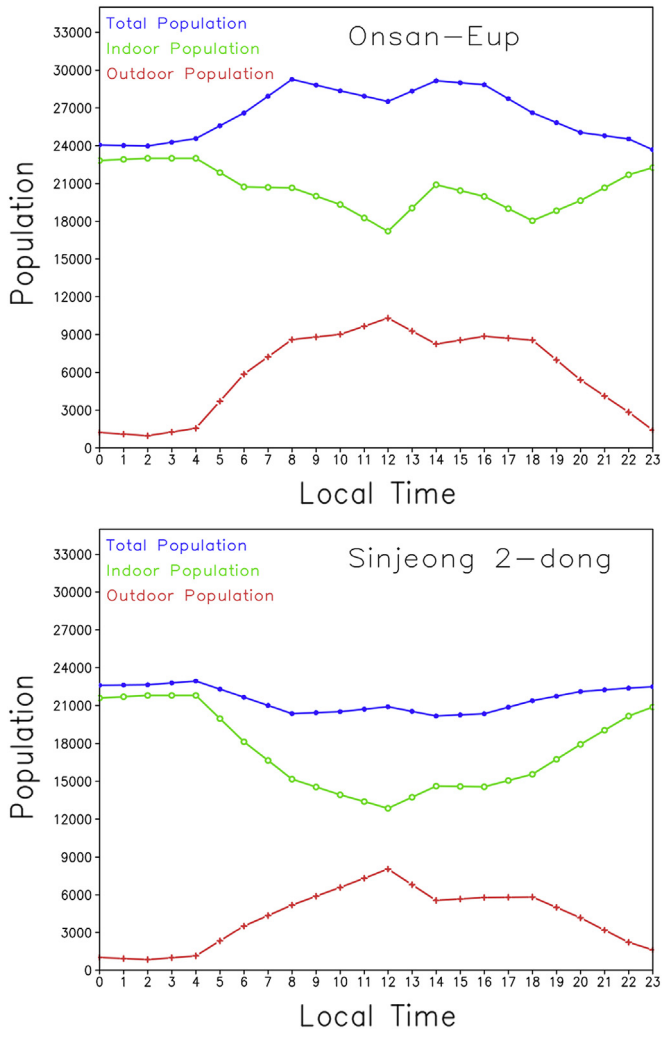

Fig. 9. Hourly total (blue), indoor (green), and outdoor (red) population variations in Onsan-Eup (upper) and Sinjeong 2-dong (lower). (For interpretation of the references to colour in this figure legend, the reader is referred to the web version of this article.)

accounts for the urban-rural temperature difference by increasing the turbulence above the rural SBL turbulence (Alan et al., 2005). In general, urban surfaces cool at slower rates than rural surfaces after sunset because buildings in urban areas trap the outgoing thermal radiation and the urban subsurface has a larger thermal capacity. Artificial heat generated by urban energy consumption also increases the nighttime urban temperature. An upward surface heat flux exists in the nocturnal urban boundary layer, increasing the mixing layer height. AERMOD defines the mixing height of the nighttime urban boundary layer as a function of the population. No concentration difference was observed between the simulations, as AERMOD does not consider the urban heat island impact during the daytime.

3.3. High concentration probability estimation

This section discusses the 1-h concentration differences between the daytime and nighttime cases based on long-term AERMOD simulation with different atmospheric conditions in August 2009 to 2013. Fig. 7 compares the 1-h concentration spatial distributions from the daytime and nighttime simulations. In addition, time-averaged concentration spatial distributions of all 155 runs are compared with the highest concentration distribution from the entire history of each independent 1-h concentration (i.e., the single highest concentration out of 155 samples) at each grid point. This pattern is used to conduct an environmental impact analysis via AERMOD. The daytime averaged concentrations suggest that the immediate vulnerable areas are approximately 1 km and 2 km from the emission source for concentration levels of 30 μg m^{-3} and 5 μg m^{-3}, respectively. The downtown areas located to the northwest of the emission source are directly affected by the accident. The time-averaged 1-h daytime concentration above 1 μg m^{-3} reaches areas 4 km from the source. Fig. 7a illustrates an asymmetric time-averaged dispersion pattern, suggesting that the local sea breeze plays a significant role. The concentration increases to the northwest of the emission source owing to a prevailing southeasterly wind (Fig. 3a). The time-averaged nighttime pattern is broader than the daytime pattern, where the average 1-h concentration above 1 μg m^{-3} reaches areas 10 km from the emission source. High concentrations are expected to the northeast and southeast of the source. The immediate vulnerable areas are located 1 km and over 3 km from the source for concentration levels of 30 μg m^{-3} and 5 μg m^{-3}, respectively. Thus, nighttime dispersion is more prevalent than daytime dispersion and can affect a larger area. The time-averaged nighttime pattern (Fig. 7b) exhibits significant spatial variation, as the nighttime wind becomes relatively weak with no preferred direction (Fig. 3b). Thus, high potential risk areas are more difficult to predict during the nighttime.

The highest concentration spatial distributions display a symmetric pattern around the emission source during the daytime and nighttime. The highest concentration distribution is not associated with the prevailing wind. These distributions may not be appropriate for identifying the potential high risk regions influenced by toxic chemical emissions. Thus, this study uses the time-averaged concentration patterns to construct the risk map.

Spatial probability distribution maps were created for the daytime and nighttime event 1-h concentrations for the three different concentration levels. As seen in Fig. 8, the daytime and nighttime simulated dispersion patterns are nearly identical to the time-averaged concentration distribution in Fig. 7. The daytime high concentration probability is highest to the northwest, corresponding to the sea-breeze regime in the study area. The nighttime result suggests that the accident affects a larger area and spreads farther from the emission source.

3.4. Risk assessment

This sub-section estimates the exposure risk to toxic benzene based on the number of people affected by the accidental exposure. The urban population significantly varies throughout the day and substantial temporal variations exist across regions owing to differing life and business behaviors. Fig. 9 highlights these differences by comparing daytime population variation patterns between Onsan-Eup and Sinjeong 2-dong, which represent the suburban industrial area and downtown residential area, respectively. The total, indoor and outdoor population time series are presented in separate figures. The indoor population represents the total number of individuals that remain inside buildings. The outdoor population represents the total number of individuals outside buildings. The total population is the sum of the indoor and outdoor populations. The indoor population of Sinjeong 2-dong decreases from 0500 LST until noon, whereas as the outdoor population increases during that period. This trend reverses from the afternoon until midnight. The total population in Sinjeong 2-dong remains relatively table, but slightly decreases between 0500 and 1900 LST. The total population decrease during the daytime hours is likely related to commuters who work in different areas. This scenario effectively represents the typical residential and business patterns of downtown areas. The Onsan-Eup population trends are

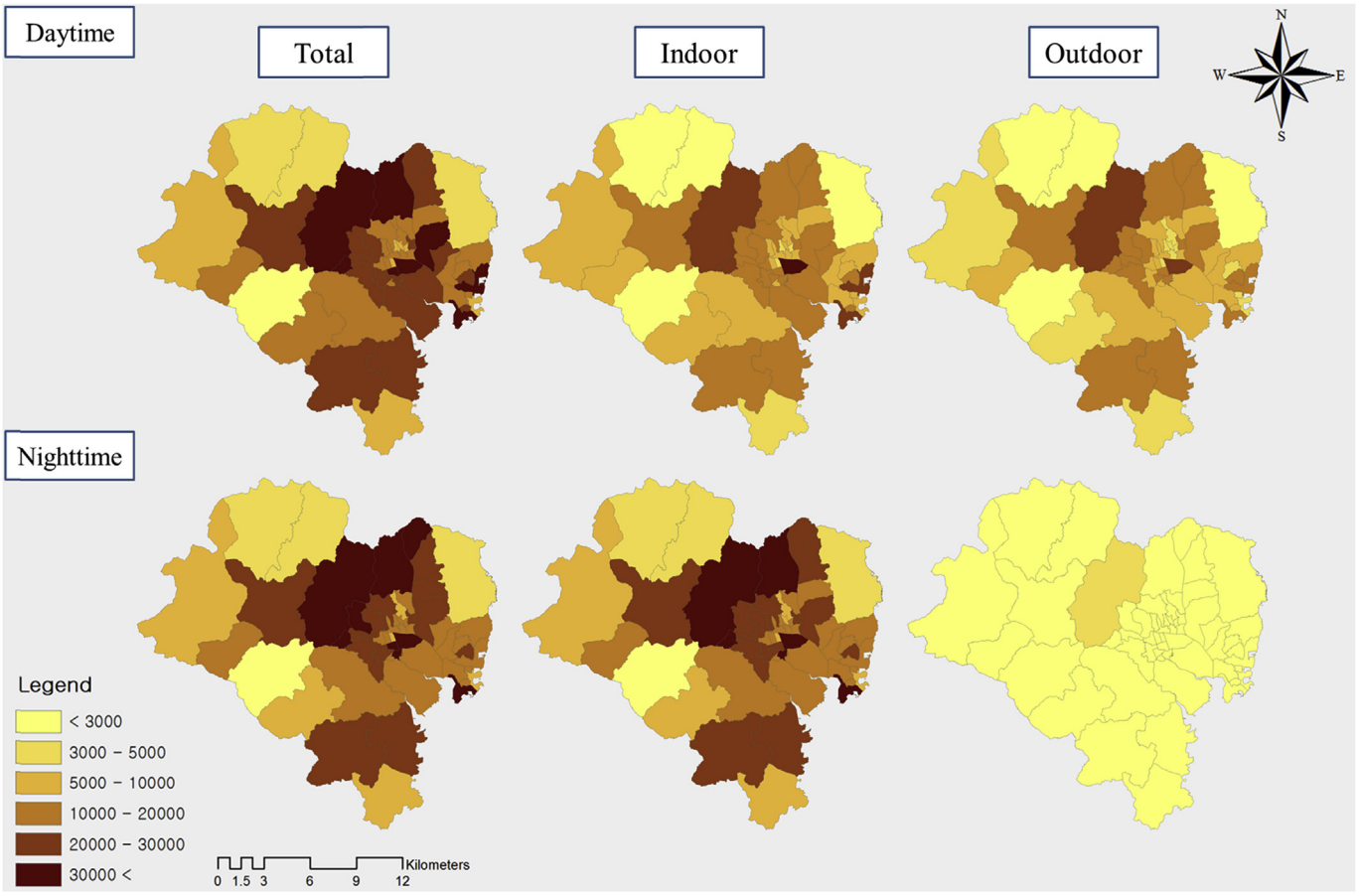

Fig. 10. Total (left), indoor (middle) and outdoor (right) population distributions in each submunicipal level administrative division. The upper panels indicate the daytime population at 1300 LST, while the lower panels illustrate the nighttime population at 0100 LST.

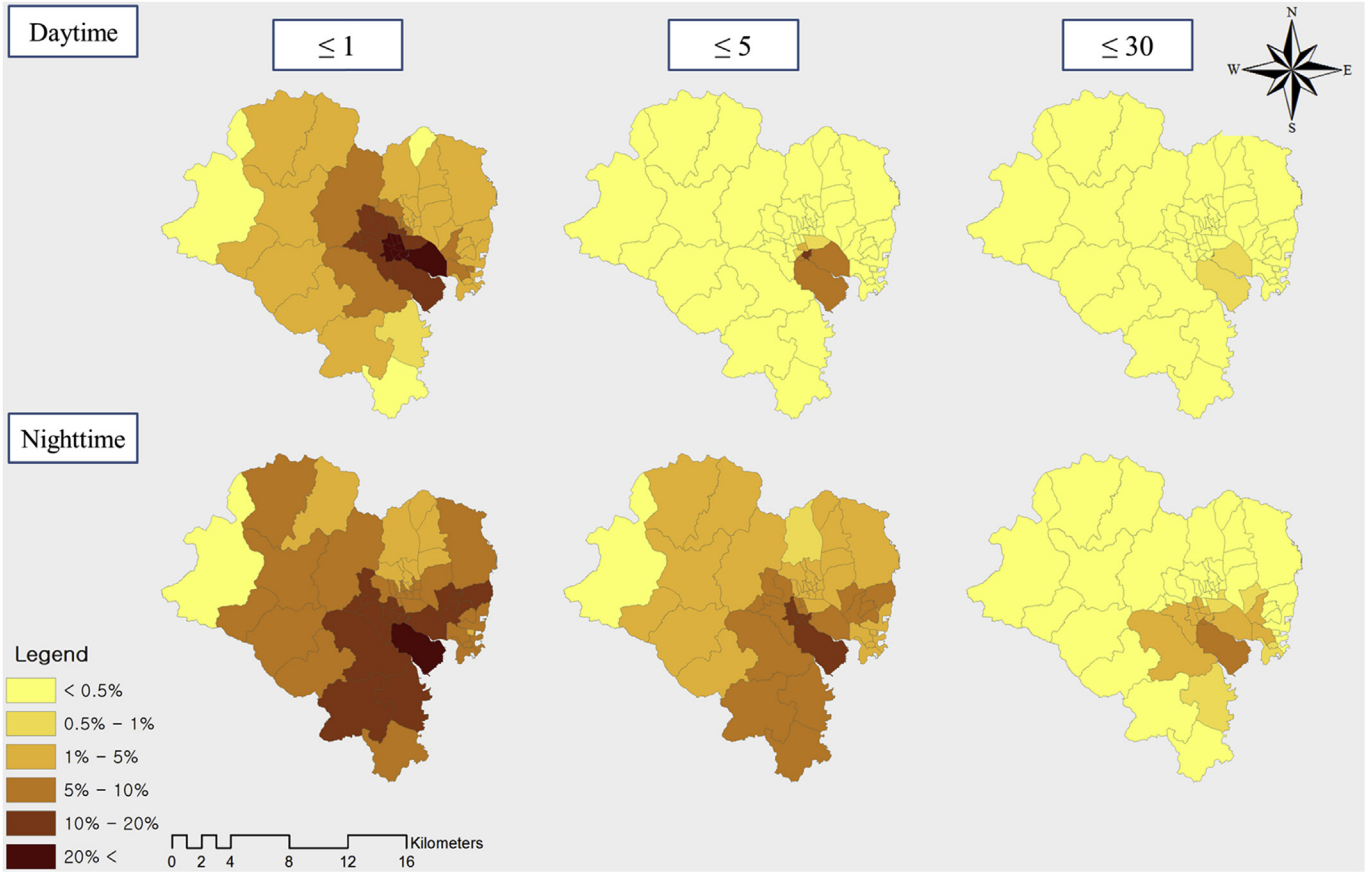

Fig. 11. Concentration probability distributions for 1 (left), 5 (middle) and 30 μg m^{-3} (right) in each submunicipal level administrative division. The upper panels indicate the daytime case at 1300 LST, while the lower panels illustrate the nighttime case at 0100 LST. The values are shown as the probability percentage.

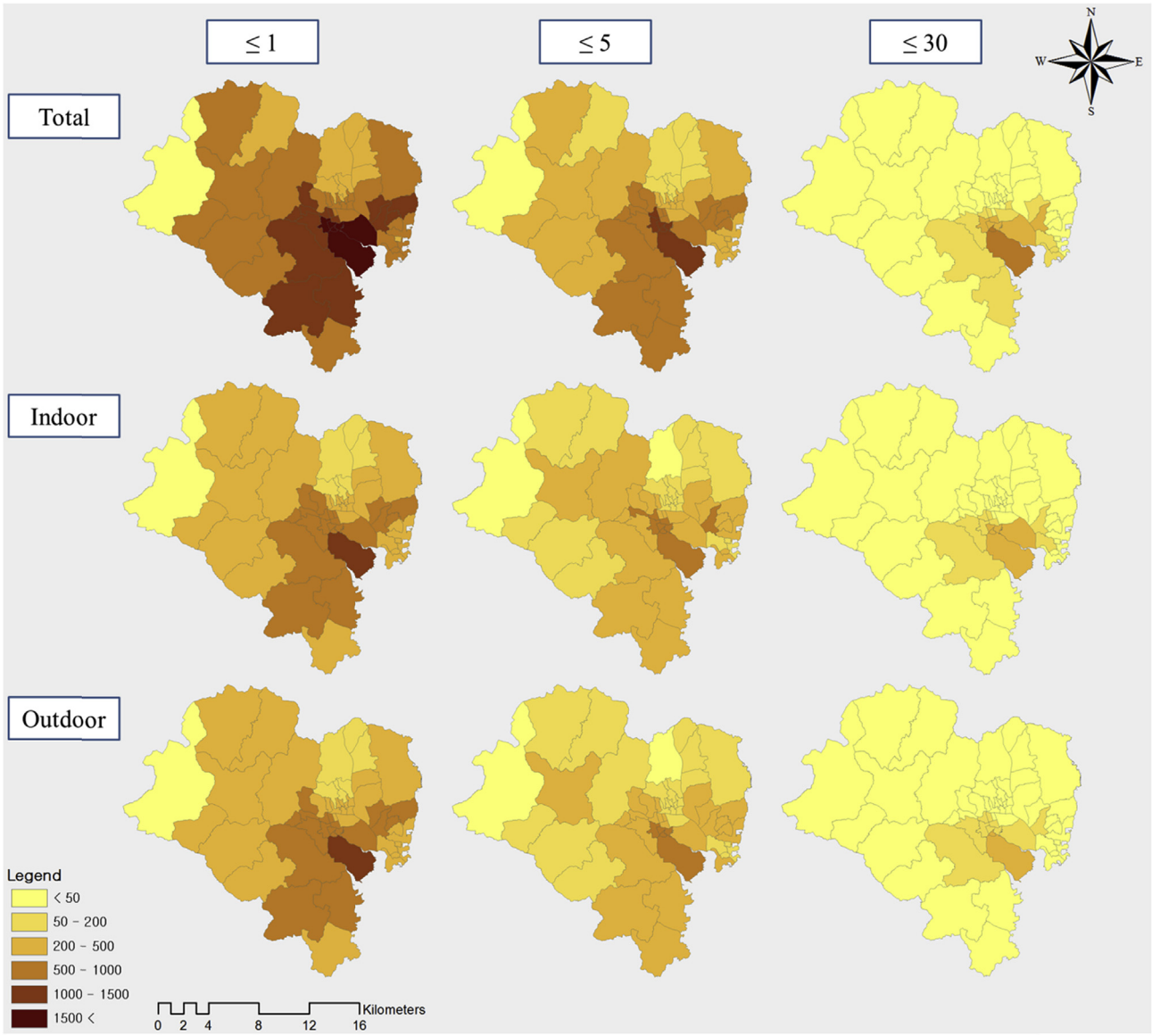

Fig. 12. Distributions of affected individuals in each submunicipal level administrative division during the daytime (1300 LST). From top to bottom, the figures present the total, indoor and outdoor population estimates for the 1 (upper panels), 5 (middle) and 30 μg m^{-3} (lower) concentrations, respectively.

moderately different than the Sinjeong 2-dong trends. The outdoor population of Onsan-Eup increases during the daytime, increasing the total population. This trend is likely related to commuting patterns to and from this industrial area. The total population of the region increases despite a decrease in the daytime indoor population, suggesting a migration of individuals from other regions. Fig. 9 illustrates that the urban population dynamically changes throughout the day, with complicated variations across different regions. This study suggests that the spatial and temporal indoor and outdoor population variations be taken into account to provide realistic estimates of the number of people affected by an accidental chemical release.

Spatial population maps were created to estimate the benzene dispersion risks at 1300 and 0100 LST. Fig. 10 illustrates the population distributions in each submunicipal administrative division. The total daytime and nighttime populations are similar in most areas, whereas the indoor and outdoor populations significantly vary. The number of people working inside and outside during the daytime is roughly equal. However, it is not surprising that most people stay inside during the nighttime. Fig. 11 presents the concentration probability distributions for 1, 5 and 30 μg m^{-3} in each submunicipal level administrative division. These results are the same as those presented in Fig. 8 expect the benzene dispersion probability is presented by averaging the probability of each administrative division. The probability decreases as the distance from the emission source increases.

Figs. 12 and 13 illustrate the distributions of individuals affected by the accident at 1300 LST and 0100 LST, respectively. The number of exposed individuals is quite similar between the daytime and nighttime for an accident probability over 1 μg m^{-3}. However, compared to the nighttime scenario in Fig. 13, the number of exposed individuals indoors is significantly larger than the number of individuals outdoors. A higher number of exposed individuals are also observed for the total nighttime population. For accident probabilities over 5 and 30 μg m^{-3}, the nighttime scenario exhibits a higher number of exposed individuals based on the total and indoor populations. However, the daytime population migration leads to a larger number of individuals exposed based on the

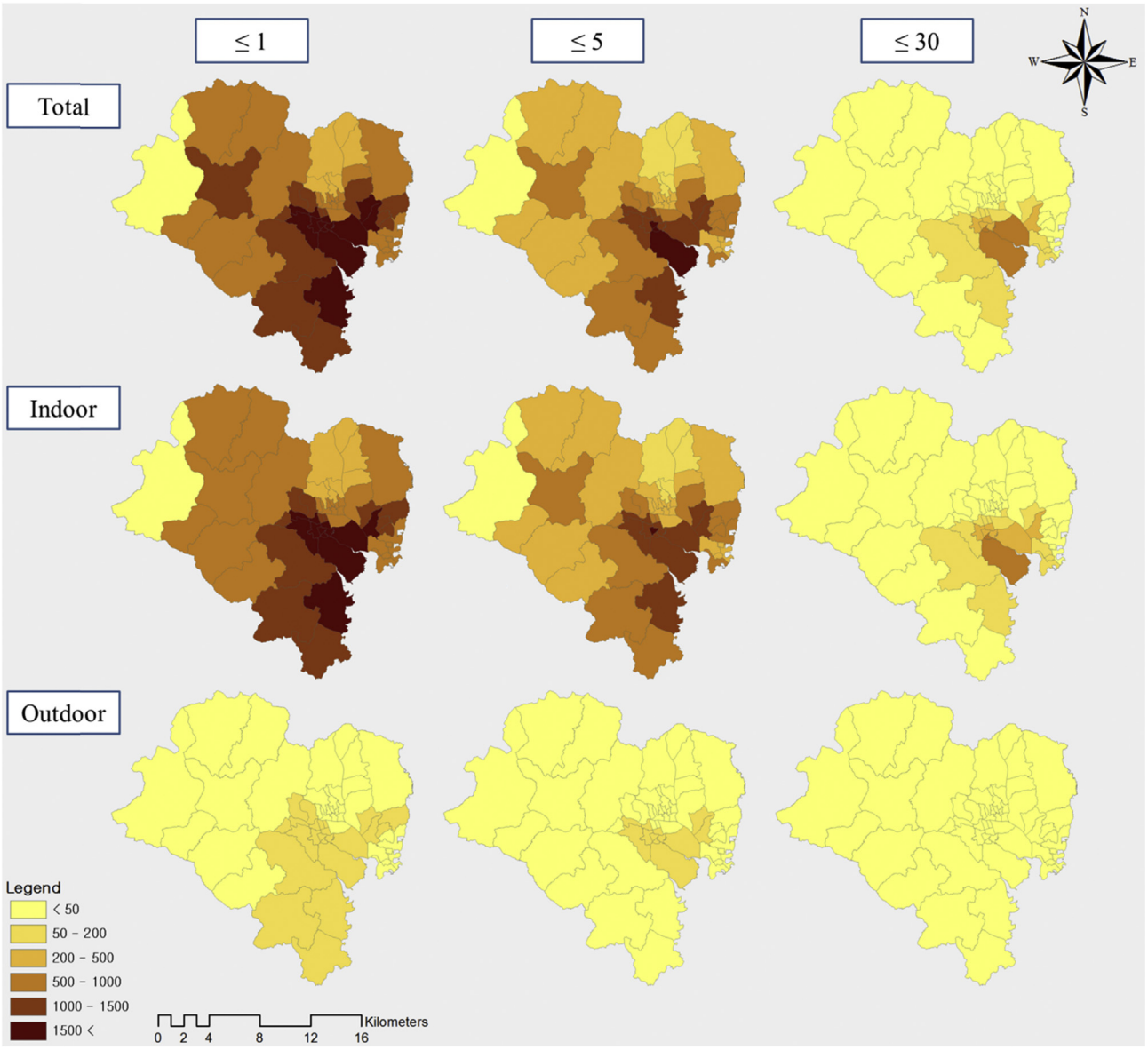

Fig. 13. Distributions of affected individuals in each submunicipal level administrative division during the nighttime (0100 LST). From top to bottom, the figures present the total, indoor and outdoor population estimates for the 1 (upper panels), 5 (middle) and 30 μg m^{-3} (lower) concentrations, respectively.

outdoor population. Thus, an accident is expected to affect fewer people if it occurs during the nighttime because most people remain inside. Conversely, a daytime accident is expected to affect more people owing to the higher outdoor population.

4. Summary and conclusions

This study used a simple Gaussian atmospheric dispersion model, AERMOD, to investigate the toxic benzene dispersion associated with an accident in the Ulsan metropolitan city. The analysis compared daytime and nighttime accident scenarios on a typical summer day. Multiple dispersion simulations were conducted using different meteorological conditions obtained from August observations between 2008 and 2013. The benzene dispersion characteristics significantly depend on the regional wind magnitude, wind direction and atmospheric stability. Long-term average dispersion patterns were used to identify the impacts of local daytime and nighttime land-sea breeze circulation trends. The atmospheric stability affected the surface concentrations by modulating turbulence and vertical diffusion.

The southeasterly sea breeze caused high daytime concentration areas to the northwest of the emission source. The high nighttime concentration areas were observed over a much larger area and in various directions from the source. The nocturnal land breeze is much weaker and non-directional, while the daytime sea breeze is relatively well-defined and regular. A larger region was affected by the nighttime accident owing to the increased atmospheric stability and decreased turbulence and vertical diffusion.

The spatiotemporal population distribution was used to quantify the accident risk, which was defined based on the number of people affected by the chemical gas accident. The spatiotemporal population distribution was estimated for each given hour of a day in 56 submunicipal administrative divisions in Ulsan. The population distributions included the total, indoor and outdoor populations. These data were based on daily empirical survey data. The potential accident risk is much larger during the daytime owing to the increase in the outdoor population. A nighttime accident is expected to affect fewer people because the majority of the

population is inside.

Even though this study focused on benzene dispersion, it provides a general modeling framework for quantifying the risks associated with arbitrary accidents for any chemical species. In particular, this study includes dynamic spatial and temporal population variations, which are important factors that should be included when assessing short-term toxic gas dispersion and inhalation risks. These population distribution patterns and results can be used by environmental impact analyses, urban planners and decision-making systems to mitigate chemical accident damages.

Note that risk quantification based on indoor and outdoor populations may facilitate appropriate evacuation policies and impact other decisions developed by local or national authorities. These policies also depend on the type of accident. Staying indoors is an effective way to minimize exposure during small, one-time chemical release events that are quickly contained. It is reasonable to suggest that the risk level of the outdoor population is much higher than that of the indoor population during such events. However, indoor populations experience the same risk as outdoor populations during large or long-term chemical release events that require lengthy recovery procedures. Therefore, the separation of indoor and outdoor population risks becomes less meaningful.

All atmospheric dispersion models possess limitations. For example, the Gaussian AERMOD may not be appropriate for long-range transport. The major disadvantage of AERMOD is that it assumes spatially uniform meteorological conditions, which may rarely occur in reality and may not be ideal for larger computational domains. Moreover, the model provides an equilibrated concentration distribution for a given atmospheric condition that is independent of temporal variations. Therefore, the dispersion plume has no memory of previous time steps. In this context, this type of simple atmospheric dispersion model may be appropriate for short-term dispersion applications over small areas, such as in this case study. Models are critical for short-duration, small-scale hazardous release events when forecasters must quickly input local weather conditions and initial accident report parameters into various dispersion models and then provide the best available results and risk information to local stakeholders and decision makers.

Acknowledgments

This research was supported by the UMI Research Fund [1.140017.01] of UNIST (Ulsan National Institute of Science and Technology).

References

Alan, J.C., Steven, G.P., Akula, V., Jeffrey, C.W., Robert , J.P., Robert, B.W., Russell, F.L., Warren, D.P., Roger, W.B., 2005. AERMOD: a dispersion model for industrial source applications. Part I: general model formulation and boundary layer characterization. J. Appl. Meteor. 44, 682–693. http://dx.doi.org/10.1175/JAM2227.1.

Ambient Air Quality Directive, 2008. Directive 2008/50/ec of the European Parliament and of the Council of 21 May 2008 on Ambient Air Quality and Cleaner air for Europe.

Amit, P., Mohit, D., Akshara, K., Ajay, O., 2007. Coupling of the Weather Research and Forecasting Model with AERMOD for pollutant dispersion modeling. A case study for PM_{10} dispersion over Pune, India. Atmos. Environ. 41 (9), 1976–1988. http://dx.doi.org/10.1016/j.atmosenv.2006.10.042.

Andler, M., Jane, M., Ilias, M., Neyval, C., 2012. Modelling of odour dispersion around a pig farm building complex using AERMOD and CALPUFF. Comparison with wind tunnel results. Build. Environ. 56, 8–20. http://dx.doi.org/10.1016/j.buildenv.2012.02.017.

Arthur, R.S., 2014. Performance evaluation of AERMOD, CALPUFF, and legacy air dispersion models using the Winter Validation Tracer Study dataset. Atmos. Environ. 89, 707–720. http://dx.doi.org/10.1016/j.atmosenv.2014.02.054.

Baklanov, A., Luisa, T., MolinaMichael, G., 2016. Megacities, air quality and climate. Atmos. Environ. 126, 235–249. http://dx.doi.org/10.1016/j.atmosenv.2015.11.059.

Edward, B., 2005. The Bhopal disaster and its aftermath: a review. Environ. Health 4 (6). http://dx.doi.org/10.1186/1476-069X-4-6.

Gurjar, B.R., Jain, A., Sharma, A., Agarwal Gupta, P., Nagpure, A.S., Lelieveld, J., 2010. Human health risks in megacities due to air pollution. Atmos. Environ. 44 (36), 4606–4613. http://dx.doi.org/10.1016/j.atmosenv.2010.08.011.

Hadlocon, L.S., Zhao, L.Y., Bohrer, G., Kenny, W., Garrity, S.R., Wang, J., Wyslouzil, B., Upadhyay, J., 2015. Modeling of particulate matter dispersion from a poultry facility using AERMOD. J. Air & Waste Manage. Assoc. 65 (2), 206–217. http://dx.doi.org/10.1080/10962247.2014.986306.

Hang, T.N., Kim, K.H., Park, C., 2015. Long-term trend of NO_2 in major urban areas of Korea and possible consequences for health. Atmos. Environ. 106, 347–357. http://dx.doi.org/10.1016/j.atmosenv.2015.02.003.

Hasson, A.S., Segun, O.O., Steven, T., Shawn, A., Kenwood, S., Julie, S., Catalina, O., Srikar, M., Kennedy, V., Austen, S., Laxmi, R.A., Lucien, N., 2013. NOx emissions from a Central California dairy. Atmos. Environ. 70, 328–336. http://dx.doi.org/10.1016/j.atmosenv.2013.01.011.

Holmes, N.S., Morawska, L., 2006. A review of dispersion modelling and its application to the dispersion of particles: an overview of different dispersion models available. Atmos. Environ. 40 (30), 5902–6028. http://dx.doi.org/10.1016/j.atmosenv.2006.06.003.

Huang, P., Zhang, J., 2015. Facts related to August 12, 2015 explosion accident in Tianjin, China. Proc. Saf. Prog. 34 (4), 313–314. http://dx.doi.org/10.1002/prs.11789.

Kakosimos, K.E., Assael, M.J., Katsarou, A.S., 2011. Application and evaluation of AERMOD on the assessment of particulate matter pollution caused by industrial activities in the Greater Thessaloniki area. Environ. Technol. 32 (6), 593–608. http://dx.doi.org/10.1080/09593330.2010.506491.

Kanyanee, S., Vanisa, S., Kraichat, T., Anchaleeporn, W.L., 2011. Application of the AERMOD modeling system for environmental impact assessment of NO_2 emissions from a cement complex. J. Environ. Sci. 23 (6), 931–940. http://dx.doi.org/10.1016/S1001-0742(10)60499-8. http://dx.doi.org/.

Lee, K., Kwon, H., Cho, S., Kim, J., Moon, L., 2015. Improvements of safety management system in Korean chemical industry after a large chemical accident. J. Loss. Prev. Proc. 42, 6–13. http://dx.doi.org/10.1016/j.jlp.2015.08.006.

Lim, H.-S., Lee, K., 2012. Health care plan for hydrogen fluoride spill, Gumi, Korea. J.Korean Med. Sci. 27, 1283–1284. http://dx.doi.org/10.3346/jkms.2012.27.11.1283.

Marcelo, C., Marcelo, G., Miguel, S., 2003. Intercomparison of atmospheric dispersion models. Atmos. Environ. 37 (18), 2435–2449. http://dx.doi.org/10.1016/S1352-2310(03)00201-2.

Mark, R.T., Alberto, S.C., Antonio, V., Mark, A.S., 2015. Suitability and uncertainty of two models for the simulation of ammonia dispersion from a pig farm located in an area with frequent calm conditions. Atmos. Environ. 102, 167–175. http://dx.doi.org/10.1016/j.atmosenv.2014.11.056.

Mutahharah, M.M., Mimi, H.H., Rozainee, M.T., 2014. Health risk assessment of emissions from a coal-fired power plant using AERMOD modeling. Proc. Saf. Environ. Prot. 92 (5), 476–485. http://dx.doi.org/10.1016/j.psep.2014.05.008.

Nicole, H., Nicholas, R., Heileen, H., Susan, H., Mark, M., George, W., Tong, Z., Allan, B., Daniel, B.R., John, V., 2011. Estimating historical atmospheric mercury concentrations from silver mining and their legacies in present-day surface soil in Potosí, Bolivia. Atmos. Environ. 45 (40), 7619–7626. http://dx.doi.org/10.1016/j.atmosenv.2010.10.009.

Park, S.B., 2013. Alert over South Korea toxic leaks. Nature 494, 15–16. http://dx.doi.org/10.1038/494015a.

Park, J.-H., Shin, M., Cho, G.-H., 2016. A dynamic estimation of casualties from an earthquake based on a time-use survey: applying HAZUS-MH software to Ulsan, Korea. Nature Hazard 81 (1), 289–306. http://dx.doi.org/10.1007/s11069-015-2079-x.

Perry, S.G., Cimorelli, A.J., Paine, R.J., Brode, R.W., Weil, J.C., Venkatram, A., Wilson, R.B., Lee, R.F., Peters, W.D., 2005. AERMOD: a dispersion model for industrial source applications. Part II: model performance against 17 field study databases. J. Appl. Meteorol 44, 694–708. http://dx.doi.org/10.1175/JAM2228.1.

Silverman, K.C., Tell, J.G., Sargent, E.V., Qiu, Z., 2007. Comparison of the industrial source complex and AERMOD dispersion models: case study for human health risk assessment. J. Air & Waste Manage. Assoc. 57 (12), 1439–1446. http://dx.doi.org/10.3155/1047-3289.57.12.1439.

Tartakovsky, D., Broday, D.M., Stern, E., 2013. Evaluation of AERMOD and CALPUFF for predicting ambient concentrations of total suspended particulate matter (TSP) emissions from a quarry in complex terrain. Environ. Pollut. 179, 138–145. http://dx.doi.org/10.1016/j.envpol.2013.04.023.

Tartakovsky, D., Broday, D.M., Stern, E., 2016. Dispersion of TSP and PM_{10} emissions from quarries in complex terrain. Sci. Total Environ. 542 (A), 946–954. http://dx.doi.org/10.1016/j.scitotenv.2015.10.133.

Tseng, J.M., Liu, M.Y., Chang, R.H., Su, J.L., Shu, C.M., 2008. Emergency response plan of chlorine gas for process plants in Taiwan. J. Loss. Prev. Proc. 21 (4), 393–399. http://dx.doi.org/10.1016/j.jlp.2008.01.006.

UNWUP, 2014. World Urbanization Prospects - the 2014 Revision. United Nations, New York. http://esa.un.org/unpd/wup/Highlights/WUP2014-Highlights.pdf.

U.S. Environmental Protection Agency, 2005a. 40 CFR, Part 51, Appendix W. Revision to the Guideline on Air Quality Models, 68 FR 68235–68236, November 9, 2005.

WHO, 2000. Benzene. In: Air quality guidelines for Europe, second ed. World Health Organization Regional Office for Europe, Copenhagen http://www.EURO.who.int/_data/assets/pdf_file/0005/74732/E71922.pdf.